Appl Biochem Biotechnol (2012) 167:2023–2038
DOI 10.1007/s12010-012-9711-y

Amperometric Vitamin C Biosensor Based on the Immobilization of Ascorbate Oxidase into the Biocompatible Sandwich-Type Composite Film

Yangping Wen · Jingkun Xu · Ming Liu · Dong Li · Haohua He

Received: 8 November 2011 / Accepted: 23 April 2012 /
Published online: 29 May 2012

Abstract Ascorbate oxidase (AO), a biologically active macromolecule, was successfully immobilized into a biocompatible sandwich-type composite film for developing the vitamin C (VC) biosensor, and the content of VC in commercial juices was amperometrically determined. The biocompatible and conducting poly(3,4-ethylenedioxythiophene) composite film and highly stable and selective multiwalled carbon nanotubes –Nafion composite film were prepared as inner and outer films of biosensor. AO molecules were immobilized between these two composite films. The as-fabricated biosensor displayed an excellent bioelectrocatalytic performance towards the oxidation of VC, a fast current response, a low working potential, a high sensitivity, a wide linear range, and a low detection limit. Moreover, the working mechanism of the biosensor was proposed, and its kinetics was also discussed. In addition, the specificity, reproducibility, and feasibility of the as-fabricated biosensor were also evaluated. Good results of the VC determination in commercial juices indicated that the as-fabricated biosensor was a potential candidate for the electrochemical determination of VC in agricultural crops. Inner and outer films provided a promising platform for the immobilization of biologically active species.

Keywords Enzyme Immobilization · Ionic liquid microemulsions · Ascorbate oxidase · Vitamin C · Conducting polymers · Biosensor

Electronic supplementary material The online version of this article (doi:10.1007/s12010-012-9711-y) contains supplementary material, which is available to authorized users.

Y. Wen · J. Xu (✉) · M. Liu · D. Li
Jiangxi Key Laboratory of Organic Chemistry, Jiangxi Science and Technology Normal University, Nanchang 330013, People's Republic of China
e-mail: xujingkun@tsinghua.org.cn

Y. Wen · M. Liu · D. Li · H. He (✉)
Key Laboratory of Crop Physiology, Ecology and Genetic Breeding, Ministry of Education, and Key Laboratory of Physiology, Ecology and Cultivation of Double Cropping Rice, Ministry of Agriculture, College of Agronomy, Jiangxi Agricultural University, Nanchang 330045, People's Republic of China
e-mail: hhhua64@163.com

Introduction

Recent trends of biosensors have been extensively reported in the development of new biomaterials and improvement of diverse biosensor techniques. Conducting polymers (CPs) and carbon nanomaterials are an ideal biomaterial for the immobilization of biologically active species, such as organism, tissue, cell, and biologically active molecules, and rapid electron transfer in the design and improvement of the biosensor interface [1–4]. Recently, composite materials based on the integration of CPs, carbon nanomaterials, and other materials, which were supposed to possess properties of individual components with a synergistic effect on the performance of biosensors, have gained growing interest.

Poly(3,4-ethylenedioxythiophene) (PEDOT) is one of the most stable CPs available today because of its high electrical conductivity, environmental stability, and biocompatibility with biologically active species, ease of preparation, and controllable surface properties [5–8]. This imply that PEDOT as an excellent electrode modified material is a promising candidate for application in chem/biosensing devices. Nonetheless, the electrosynthesis of PEDOT is generally performed in traditional organic solutions resulting from the very low water solubility of its monomer 3,4-ethylenedioxythiophene (EDOT), which limit its application in many different fields, including fermentation, food, medicine, life science, and agriculture, in which many biologically active species require a good aqueous environment to retain their bioactivity. Previous studies have indicated that surfactants could improve properties of EDOT, such as increasing the water solubility, lowering onset oxidation potential, and stabilizing cation radical ($EDOT^{+\bullet}$), thus facilitating the formation of high-quality PEDOT film. Moreover, surfactants could also enhance the enzymatic activity and prolong the lifespan of enzyme-based biosensing devices [9–11]. In our previous studies, a biocompatible and low-toxicity amino-acid-based anionic surfactant sodium *N*-lauroylsarcosinate (SLS), which can integrate the polar amino acid group (hydrophilic moiety) and the nonpolar fatty acid long-chain (hydrophobic moiety), and create an amphiphilic structure with high surface activity, physicochemical, and biological properties [12–14], could enhance the biocompatibility of the resultant PEDOT film by forming the PEDOT-SL film [15].

More recently, the electrosynthesis and behavior of PEDOT in various pure ionic liquids (ILs) system have been studied [16–20], and their properties and applications in chem/biosensing devices have also been reported. These biosensors fabricated in ILs exhibited excellent performance and good anti-interference to impurities [21, 22], which is very beneficial to the design and application of biosensors. However, water is still an excellent, non-toxic, and inexpensive solvent system compared with ILs system in the electrochemistry of PEDOT. Hence, an ionic liquid–water mixture system is an excellent, non-toxic, and cost-effective system for the electrochemistry of PEDOT by combing advantages of the two. Furthermore, the high-quality PEDOT film is easily obtained in ILs/surfactant/H_2O system [23]. In previous reports, a halogen-free and relatively hydrolysis-stable ionic liquid 1-ethyl-3-methylimidazolium ethyl sulfate (EMIES), which possesses not only interesting physicochemical properties of the most common ILs, but also a number of desirable features such as simple preparation, low cost and toxicity, hydrophilicity, and stability in air [24]. As a "green" solvent and supporting electrolyte, EMIES is now widely used for the development of highly sensitive and selective biosensors [25–27]. Moreover, EMIES-in-water is the most suitable for the electrosynthesis of the high-quality poly(3,4-ethylenedioxythiophene) (PEDOT) [28] (Fig. S1).

Multiwalled carbon nanotubes (MWCNTs), currently one of the most attractive carbon nanomaterials, have widely employed for the design of efficient biosensors because of their high surface area, excellent electrical conductivity, significant mechanical strength, good

chemical stability, and biocompatibility [29–30]. Enzyme-based biosensors based on composites with network structure of MWCNTs were beneficial to improve conductivities and mechanical properties of film, facilitate the immobilization of biologically active species and direct electron transfer, and enhance the stability of biosensors [31–34]. PEDOT–MWCNT composites not only improved the mechanical integrity, electrochemical activity, and electronic and ionic conductivity but also enhanced the stability and biocompatibility of AO-based biosensors [35, 36]. In addition, MWCNT–Nafion composites could enhance the selectivity and sensitivity of electrochemical biosensors and the interfacial adhesion of the modified electrode surface [37–39]. The main reason is that Nafion can provide a biocompatible environment for biologically active species, enhance the anti-interference ability of the chem/biosensor, prevent the leakage of biologically active species, and improve the adhesion and binding force between films and electrode interface [40, 41]. Moreover, Nafion composite electrodes were easily prepared by casting a small volume of the solution onto the electrode surface and allowing the solvent to evaporate. Resulting composites possess high adhesion to the electrode surface and low swelling in aqueous media [42, 43].

In this paper, we report the amperometric VC biosensor based on the immobilization of AO molecules into a biocompatible sandwich-type composite film. The biocompatible and conducting inner film was synthesized in ionic liquid microemulsion using the one-step potentiostaticall deposition method. The high stable and selective outer film was obtained by blending Nafion and MWCNTs together with a volume ratio of 1:1. The working mechanism and reaction kinetics of the fabricated biosensor were proposed. Finally, the as-fabricated biosensor was employed for the detection and analysis of VC in commercial juices.

Experimental

Chemicals

AO (from *Cucurbita* sp., 250 U g^{-1}), EDOT, and SLS were purchased from Aldrich. EMIES was obtained from Tokyo chemical industry Co., Ltd. Lithium perchlorate trihydrate ($LiClO_4 \cdot 3H_2O$), disodium hydrogen phosphate dodecahydrate ($Na_2HPO_4 \cdot 12H_2O$), and sodium dihydrogen phosphate dihydrate ($NaH_2PO_4 \cdot 2H_2O$) were obtained from the Sinopharm chemical reagent Co., Ltd. Phosphate-buffered solutions (PBS, 5×10^{-2} M, pH=6.5) was prepared from 5×10^{-2} M $NaH_2PO_4 \cdot 2H_2O$, and 5×10^{-2} M $Na_2HPO_4 \cdot 12H_2O$. VC was purchased from Bio Basic Inc., 5 % Nafion was obtained from DuPont Co., Ltd., 4 % MWCNTs (outer diameter, 50–100 nm; length, 5–15 μM) was purchased from Chengdu Institute of Organic Chemistry, Chinese Academy of Sciences. All reagents were of analytical grade and used without further purification. All solutions were prepared using deionized distilled water as solvent.

Fabrication of AO Composite Modified Electrode

The biocompatible and conducting inner film was one-step deposited potentiostatically on the surface of a bare glassy carbon electrode (GCE) in ionic liquid microemulsions containing 20 mM EDOT, 0.1 M EMIES, and 0.1 M SLS at a constant potential of 1.1 V vs. saturated calomel electrode (SCE) for 90 s in a one-compartment three-electrode cell (Scheme 1). The inner film was washed repeatedly with deionized distilled water to remove the electrolyte and monomer. The GCE with a diameter of 3 mm served as the working

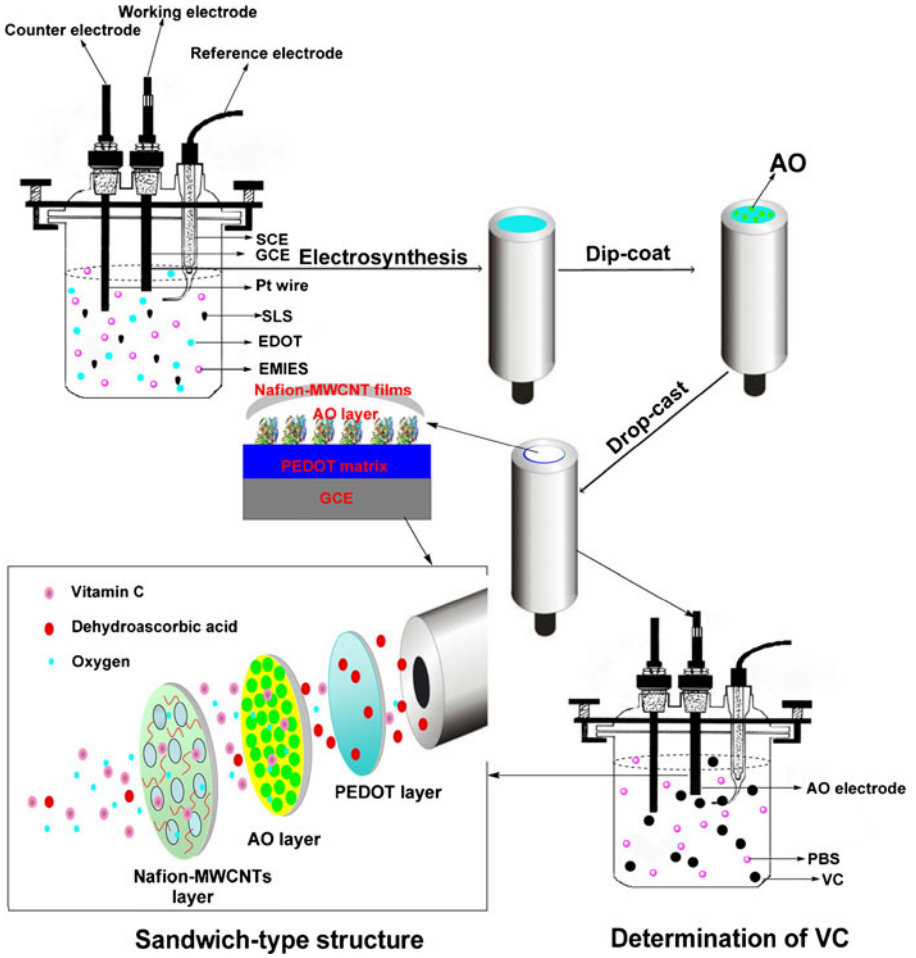

Scheme 1 The preparation and working mechanism of the fabricated sandwich-type AO composite modified electrode

electrode, and a platinum wire with a diameter of 1 mm was used as the counter electrode. The reference electrode was SCE. The counter electrode was carefully polished with abrasive paper (1,500 mesh). The GCE was polished with alumina (Al_2O_3, 0.05 μm). Then, the counter electrode and GCE were ultrasonically cleaned in turn with acetone, ethanol, and deionized distilled water each for 5 min, respectively. Then, they were dried in air before each experiment. Three electrodes in the cell were placed 5 mm apart during electrochemical measurements. All solutions (except for solutions containing VC) were deoxygenated by bubbling with dry argon for 10 min prior to each experiment. All experiments (except for those containing VC) were performed under slight argon overpressure. Unless otherwise stated, the temperature was kept at 25 °C. To prepared high stable and selective outer film, the mixture of Nafion–MWCNT was obtained by blending 5 % Nafion and 4 % MWCNTs together and stirring thoroughly for 2 h in a volume ratio of 1:1, and then this mixture was dip-casted onto the surface of enzyme layer and allowing MWCNT–Nafion composite film to air dry. Five microliters of 0.3 g L^{-1} AO was dip-coated on the surface of the

biocompatible inner film. After drying in air, 5 μL of the mixture of MWCNT–Nafion was dip-casting the surface of the AO layer, and then the high stable and selective outer film was allowed to air dry. Finally, the fabricated sandwich-type AO composite modified electrode was stored in PBS at 4 °C prior to use.

The VC Detection of the As-Fabricated Biosensor

Current–time (*I*–*t*) curves of the as-fabricated biosensor for the detection of VC were obtained by chronoamperometry at a working potential of 0.05 V vs. SCE. Steady-state response current densities (*I*) was recorded in 0.05 M PBS (pH=6.5) containing different concentrations of VC (Scheme 1). The bioelectrocatalytic performance of the biosensor towards oxidation of VC was studied by the cyclic voltammetry. Peak current densities were recorded in PBS containing different concentrations of VC at the potential scan rate of 100 mV s^{-1}.

Determination of VC in Commercial Juices

All commercial juices containing VC were purchased from a local supermarket. Different kinds of VC samples were prepared from different kinds of commercial juices containing VC and 50 mM PBS (pH=6.5). Then, these samples were kept at 4 °C in dark when not in use. Finally, all VC samples were determined using the as-fabricated biosensor. Values measured by the as-fabricated biosensor were compared to that given by manufacturers.

Apparatus

All electrochemical experiments were performed with a potentiostat–galvanostat (model 263A, EG&G Princeton Applied Research). VC samples were added with the Finnpipette (Labsystems, Helsinki, Finland). The pH value was measured with a Delta 320 pH meter (Mettler-Toledo Instrument, Shanghai, China). The temperature was controlled with a type HHS thermostat (Shanghai, China).

Results and Discussion

Surface Morphology of Fabricated Electrode

The surface morphology of the PEDOT film electrosynthesized in ionic liquid microemulsions was visualized by SEM (Fig. 1a, b). Unlike the rough and porous surface of PEDOT film obtained from traditional organic solvents, the electrosynthesized PEDOT film produced a regular and smooth, dense, compact, and homogeneous surface, which was in accordance with previous reports on the electrosynthesis of the PEDOT film in aqueous micellar systems [15, 35]; the result could be explained as a consequence of the relatively high concentration of doping anions that could stabilize with cation radical ($EDOT^{+\bullet}$) during the electropolymerization process. This led to morphological changes of the coating, giving rise to a more regular and compact structure. This surface structure of PEDOT matrix could facilitate the fast electron transfer during the bioelectrocatalytic oxidation of VC. SEM images of biologically active macromolecules AO on the surface of the PEDOT matrix are presented in Fig. 1 c and d. Obviously, AO molecules adhered tightly to the regular and smooth, dense, compact, and homogeneous surface of the PEDOT matrix, which was very

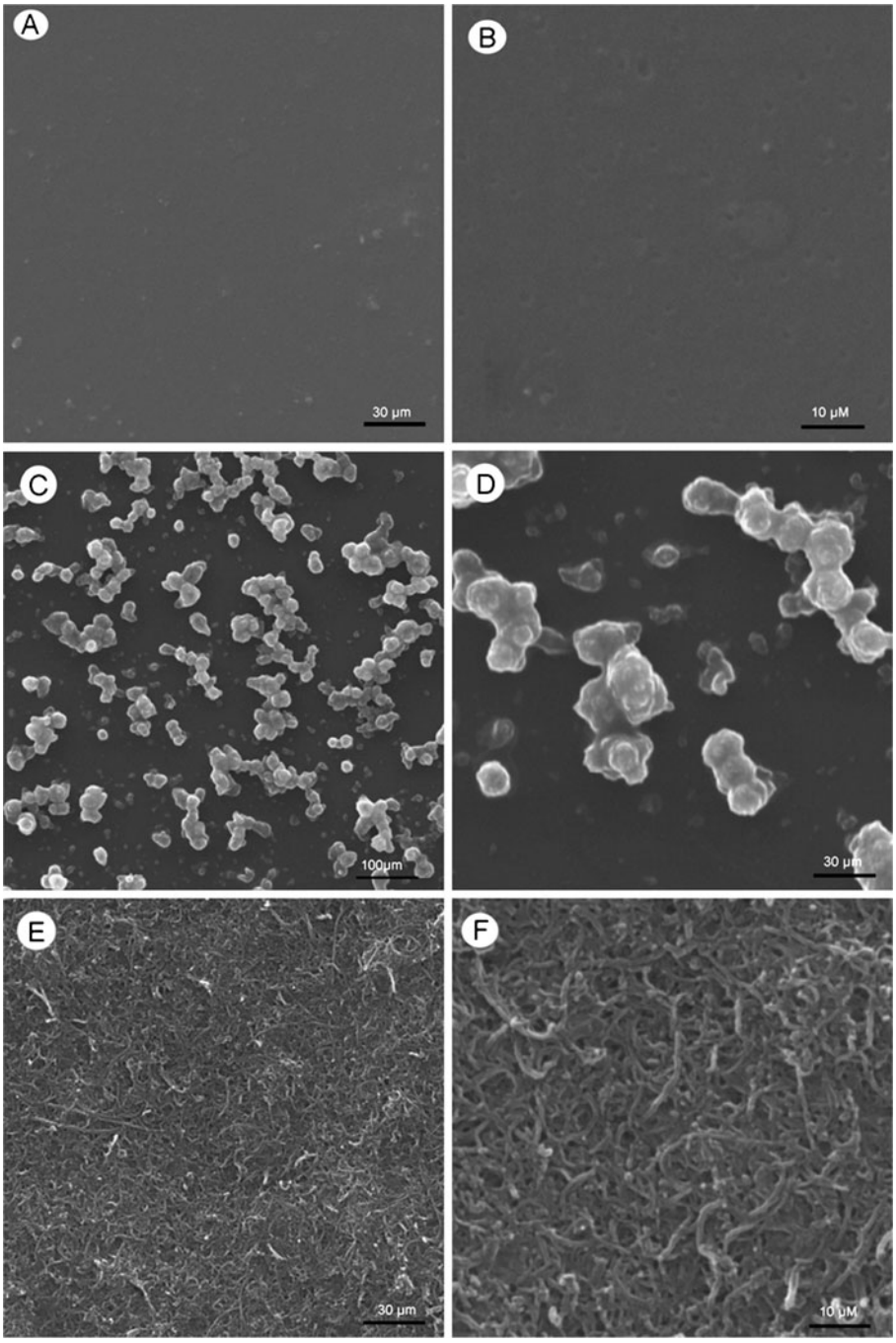

Fig. 1 SEM of PEDOT composite layer, AO layer, and Nafion-MWCNTs composite layer prepared on the surface of ITO electrodes (**a**, **d**, and **f** ×30,000 magnification), (**b** and **e** ×10,000 magnification), and (**c** ×5,000 magnification)

beneficial to the fast electron transfer from enzyme layer to the interface of PEDOT matrix. The MWCNT–Nafion film in Fig. 1e and f showed clearly that MWCNTs were well-dispersed in Nafion matrix; the formed MWCNT–Nafion composite film with rough ordered network structures was very beneficial to the attachment, diffusion, and bioelectrocatalytic oxidation of VC.

Bioelectrocatalytic Performance of AO Composite Modified Electrode

The bioelectrocatalytic performance of the fabricated sandwich-type AO composite modified electrode towards the oxidation of VC is shown in Fig. 2. It could be seen that the bioelectrocatalytic oxidation of VC began to appear from −0.1 V and reached the maximum value at approximately 0.2 V. Moreover, peak current densities gradually increased with increasing the concentration of VC, suggesting that the fabricated composite modified electrode possessed an excellent bioelectrocatalytic performance for the oxidation of VC. Moreover, the synergistic electrocatalytic effect of MWCNTs could enhance the bioelectrocatalytic performance of the AO-based biosensor [35, 36]. In addition, the oxidation peak potential of the fabricated AO composite modified electrode for the bioelectrocatalytic oxidation of VC was gradually shifted to a less-positive potential when the concentration of VC exceeded 1 mM, which ascribed to the consumption of the dissolved O_2 in surrounding enzymes.

Working Mechanism of AO Composite Modified Electrode

To study the working mechanism and reaction kinetics of the fabricated sandwich-type AO composite modified electrode, the structure and reaction mechanism of AO molecules were elucidated. AO molecules as a homodimer copper-containing enzyme belongs to the family of oxidoreductases with a molecular weight about 140 kDa containing eight copper ions, which catalyze a redox reaction between VC and O_2 (Scheme S1), and each subunit consists of three domains with four copper atoms of mononuclear and trinuclear centers. These three copper ions are bound in mutual proximity to constitute trinuclear centers between domains 1 and 3; trinuclear copper site probably represents oxygen binding and electron storage site. The remaining one copper ion constitutes mononuclear in domain 3, and mononuclear

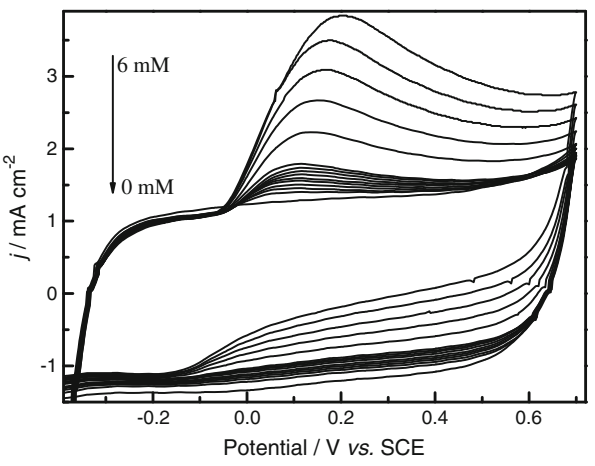

Fig. 2 The bioelectrocatalytic activity of the fabricated sandwich-type AO composite modified electrode towards the oxidation of VC

copper site probably represents VC binding site [44, 45].

Several researchers have studied the reaction mechanism of VC biocatalytic oxidation by AO [46, 47]. They revealed that enzymatic reaction occurred in the presence of two substrates (VC and O_2) and two reactants VC (first) and O_2 (second) resulting in products of dehydroascorbic acid (DHA) and H_2O, which was denoted as the double displacement reaction mechanism of enzymatic catalysis [48]. It is a two-substrate reaction; substrates appear to bounce on and off from enzyme, just like a ping-pong ball bouncing up and down on a table. Thus, this mechanism is also called as "ping-pong" reaction mechanism. Moreover, this reaction does not occur sequentially, VC first binds to free enzyme E_{ox}^{AO} and forms $VC \cdot E_{ox}^{AO}$, then transforms into E_{red}^{AO} ·DHA, next releases product DHA, and forms modifying enzyme E_{red}^{AO}. The second substrate O_2 also binds to modifying enzyme E_{red}^{AO} to form $O_2 \cdot E_{red}^{AO}$, which transforms into E_{ox}^{AO}. H_2O then releases another product H_2O and forms a free enzyme E_{ox}^{AO} again (Scheme S1B).

The working mechanism of the fabricated sandwich-type AO composite modified electrode was proposed based on the structure and reaction mechanism of AO molecules mentioned above. Firstly, AO molecules in the biocompatible conducting PEDOT composite matrix specifically recognize and bind to two reactants VC and O_2. Then, complex enzyme-catalytic reaction occurred. Meanwhile, a series of the complex biochemical signals were produced and biomagnified. These signals were captured by PEDOT composite matrix and converted into electrical signal. Finally, the electrical signals transferred to the GCE surface and were detected and recorded by a potentiostat–galvanostat under computer control. In addition, MWCNTs not only could promote the direct electron transfer between AO molecules and the matrix interface (Scheme 1) but also enhance bioelectrocatalytic oxidation of VC during electrochemical detection of VC.

Working Potential of AO Composite Modified Electrode

The effect of the working potential on the current response of the fabricated sandwich-type AO composite modified electrode is shown in Fig. 3. The current response increased rapidly in the beginning and then reached a steady state within 10 s between −0.1 and 0.05 V, indicating that the response current was controlled by the enzyme kinetics of biocatalytic reaction and the electrochemical processes. However, when the working potential above 0.05 V, response current became almost constant, indicating that the composite modified

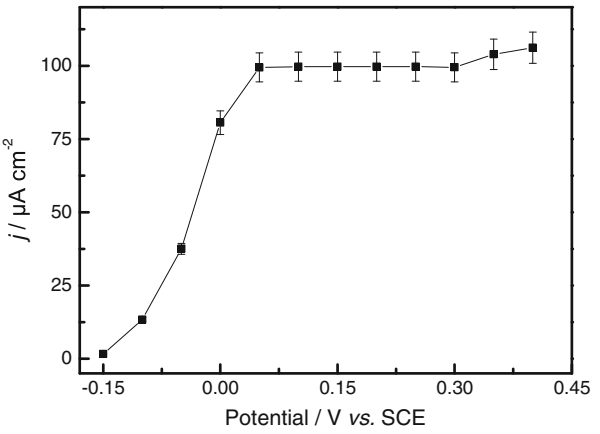

Fig. 3 Effect of working potential on the response current of the fabricated sandwich-type AO composite modified electrode

electrode response was limited by the diffusion of substrates and products. The relationship between response current and working potential in the range from 0.05 to 0.3 V showed that very little working potential dependence was observed. A very low working potential was desirable for avoiding the interference of reducing agents in real samples. Moreover, working potential in this paper was lower than that in previous studies [36, 48, 49], which was relative to the electrocatalytic activity of MWCNTs and physicochemical properties of EMIES. The introduction of conducting MWCNTs and EMIES can improve the conductivity of the resulting composite film and promote the direct electron transfer between AO molecules and the matrix interface, and MWCNTs have synergistic effect on the bioelectrocatalytic performance of the AO-based biosensor. Hence, the optimal working potential of the fabricated AO composite modified electrode was selected as 0.05 V in subsequent experiments.

Detection of VC

Figure 4 shows *I*–*t* plots of the fabricated sandwich-type AO composite modified electrode in PBS containing various concentrations of VC. Obviously, the value of *I* linearly increased with the increase in the VC concentration (Fig. 4 inset) and showed a fast current response (approximately 10 s), revealing that this method could successfully detect the unknown concentration of VC. Moreover, *I* had a linear dependence on VC concentration at lower concentration and approached an asymptotic value denoted by I_{max} (the apparent maximum steady state response current) at higher concentration (Fig. 5). Compared to recent studies [36, 48–52], the relationship between the response current and concentration of VC showed wider linear range from 4.0×10^{-7} to 1×10^{-3} M. This method had a higher sensitivity of 187 mA M^{-1} cm^{-2} (from the slope of the linear part Fig. 4) and a lower detection limit of 0.087 μM (*S*/*N*=3). The biosensing performance of the fabricated AO composite modified electrode was better than that in previous reports [36, 48–52]. In addition, the better biosensing performance indicated that the biocompatible and conducting PEDOT composite matrix and MWCNT–Nafion composite film might improve sensitivity and stability of biosensing devices. When the concentration of VC was higher than 1 mM, the curve exhibited a gradual deviation from linearity (Fig. 5). The main reason was that the excess consumption of O_2 dissolved in surrounding enzymes resulted in the lower efficiency of

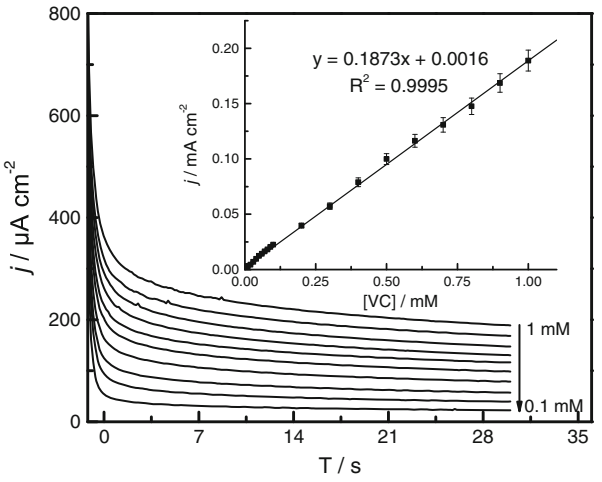

Fig. 4 The relationship between the response current and concentration of VC. *Inset* The linear portion of VC concentration range

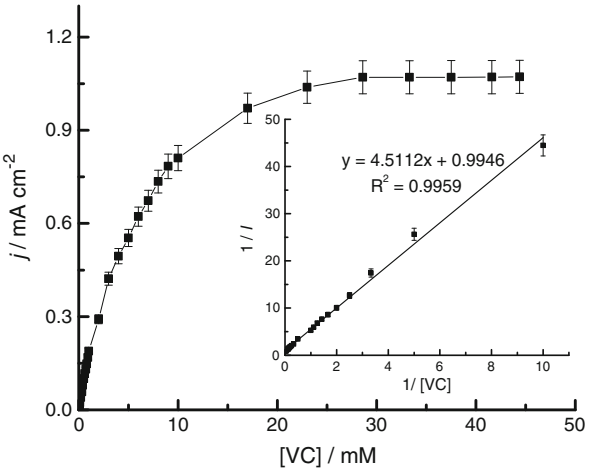

Fig. 5 Line weaver–Burk plots of the fabricated sandwich-type AO composite modified electrode under optimal parameter conditions

enzymatic catalysis due to the insufficient O_2 during the enzymatic reaction. Moreover, AO was gradually saturated with the increasing concentration of VC at very high concentration. Consequently, the response current of the fabricated AO composite modified electrode gradually achieved constant (I_{max}) due to the gradual equilibrium of enzymatic reactions. The response time was below 10 s at lower VC concentration and gradually lengthened with the increasing concentration of VC due to the insufficient O_2 dissolved resulting in the very slow reaction velocity (V) of the two-substrate enzymatic catalysis.

Kinetics of AO Composite Modified Electrode

Kinetics of the fabricated sandwich-type AO composite modified electrode was investigated in detail according to the double displacement reaction mechanism and the steady-state assumption of enzymatic catalysis based on the two-substrate molecules [53–55], the two-substrate binding step was assumed to be relatively faster than the rate of breakdown of enzyme–substrate complexes. In other words, this reaction was based on the assumption that one rapid equilibrium was formed between a free enzyme $\left(E_{ox}^{AO}\right)$ and the first substrate (VC), which rapidly reacted to form the first enzyme-substrate complex $\left(VC \cdot E_{ox}^{AO}\right)$, then broke down and released the first product (DHA) and formed a modified enzyme $\left(E_{red}^{AO}\right)$; the other rapid equilibrium was formed between a modified enzyme $\left(E_{red}^{AO}\right)$ and the second substrate (O_2), which rapidly reacted to form the second enzyme–substrate complex $\left(O_2 \cdot E_{red}^{AO}\right)$, then broke down and released another product (H_2O) and formed a free enzyme $\left(E_{ox}^{AO}\right)$ (S1B). The kinetic equation (Scheme S1D) of VC and O_2 reaction catalyzed by AO molecules was obtained according to the kinetic equation of enzymatic catalysis based on two-substrate molecules (Scheme S1C) [53–55]. In the case of the electrochemical biosensor, the steady-state current (I) was instead of V, and the apparent Michaelis–Menten constant $\left(K'_{mapp}\right)$ was instead of K_m [54–57]. Hence, the equation of Scheme S1D was expressed as the equation of Scheme S1E, which also could be expressed as the equation of Scheme S1F by transformation, while K'_{mapp} and I_{max} in the equation of Scheme S1F could be expressed as equation of Scheme S1G and displayed a hyperbolic dependence on the concentration of O_2. Namely K'_{mapp} was changed with the change of the O_2 concentration, and K'_{mapp}

approached an asymptotic value denoted by K_m^{VC} when O_2 are saturated. In the same way, I_{max} was also changed with the change of the O_2 concentration, and I_{max} also approached an asymptotic value denoted by I_{max} when O_2 was saturated. Therefore, K_m^{VC} was Michaelis–Menten constant of VC when O_2 was saturated, $K_m^{O_2}$ was Michaelis–Menten constant of O_2 when VC was saturated, I_{max} was the maximum steady state current when all two substrates VC and O_2 were saturated, and $K_{mapp}^{'}$ and I_{max} were the apparent Michaelis–Menten constant and the apparent maximum steady state current for the catalyzed reaction of the fabricated AO composite modified electrode, respectively. In VC and O_2 reaction catalyzed by AO, the concentration of O_2 is held a constant, while the concentration of VC is varied in the fabricated AO composite modified electrode. Therefore, the freshly prepared VC sample solutions with different concentrations of VC were used prior to each measurement in order that the concentration of O_2 kept a constant in air-saturated buffer solution in all experiments. Moreover, the corresponding Lineweaver–Burk equation (Scheme S1H) of enzymatic catalysis could be also expressed as the equation of Scheme S1I in the fabricated AO composite modified electrode.

The determination of $K_{mapp}^{'}$ and I_{max} was obtained in experiments by Lineweaver–Burk plot of VC and O_2 reaction catalyzed by AO molecules (Fig. 5 inset). After linear regression, an equation of the form $y = A + Bx$ was obtained. The inverse of A is $I_{max}^{'}$, as at that point, x is 0, whereas $K_{mapp}^{'}$ is calculated as $B\,(A)^{-1}$, as at that point, y is 0. The values of $K_{mapp}^{'}$ and I_{max} were calculated as 4.536 mM and 1.005 mA cm^{-2}, respectively. The values of $K_{mapp}^{'}$ and I_{max} were lower than that reported for the fabricated AO composite modified electrode based on PEDOT composite film [36, 49]. Michaelis–Menten constant is a measure of enzymatic affinity for its substrate and corresponds to the substrate concentration at 1/2 V_{max}. It is inversely proportional to the enzymatic affinity for its substrates. Therefore, lower values of $K_{mapp}^{'}$ indicated that the fabricated AO composite modified electrode had better bioaffinity.

Bioaffinity of Composite Modified Electrode

Enzyme molecules have limited bioactivity, especially when removed from their native microdomains. Therefore, the bioactivity of enzyme molecules decreased when it was immobilized in organic films. However, MWCNTs and EMIES could not only promote the fast electron transfer between enzyme molecules and the modified electrode interface but also avoid denaturation and inactivation of enzyme molecules during the immobilization of enzyme molecules and the use as well as storage of the fabricated sandwich-type AO composite modified electrode. Moreover, SLS, Nafion, MWCNTs, and EMIES also could improve the biocompatibility of film and weaken its toxicity, which was beneficial to enhance enzymatic activities and improve the lifespan of the AO-based biosensors.

The apparent activation energy (E_a) of the fabricated sandwich-type AO composite modified electrode was presented in Fig. 6. The ln$I$ vs. 1/T graphs depicts the relationship between the Napierian logarithm of I and the inverse of the temperature. The value of E_a was calculated by the Arrhenius equation as follows:

$$\ln k = \ln k0 - \frac{E_a}{RT} \Rightarrow \ln I = \ln I0 - \frac{E_a}{RT} \tag{1}$$

Here, I is the steady-state current response, I_0 represents a collection of currents, R is the universal gas constant, T is the absolute temperature in Kelvin, and E_a is the apparent activation energy. After linear regression, an equation of type $y = A + Bx$ was obtained, and

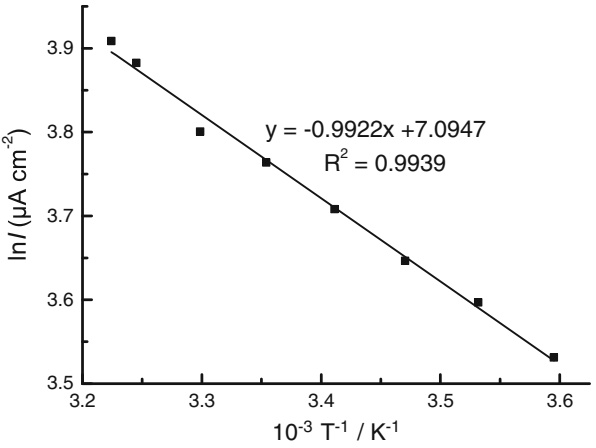

Fig. 6 The determination of E_a on the fabricated sandwich-type AO composite modified electrode

then the value of E_a was calculated from $E_a = BR$. The E_a value of the fabricated AO composite modified electrode was 8.249 kJ M^{-1}. Obviously, the value of E_a was lower than our previous studies [36, 49]. The lower value of E_a meant that the fabricated AO composite modified electrode possessed higher bioactivity and bioaffinity towards its substrate, which was in good agreement with the lower value of K'_{mapp} . The higher bioactivity and bioaffinity also indicated that MWCNT–Nafion could enhance interfacial adhesion between AO molecules and PEDOT composite modified GCE, which could effectively promote the fast electron transfer between AO molecules and the modified electrode interface.

Stability of AO Composite Modified Electrode

The repeatability and reproducibility of the sandwich-type AO composite modified electrode were very important parameters when testing its analytical performance. However, biologically active species have limited stabilities, especially when they are removed from native microdomains and immobilized in non-native matrix. Thus, the reproducibility and repeatability of the fabricated AO composite modified electrode should be investigated.

The repeatability of the fabricated AO composite modified electrode in terms of repetitive use in PBS containing 0.1 mM VC is presented in Fig. 7a. The relative standard deviation (RSD) was 1.2 % for 40 successive assays, showing a good repeatability of the fabricated AO composite modified electrode.

The reproducibility of the fabricated sandwich-type AO composite modified electrode was also evaluated via the comparison of the response current of the prepared ten AO composite electrodes. These electrodes were tested independently for the response current of the VC bioelectrocatalytic oxidation in PBS containing 0.5 mM VC, providing a RSD value of 2.17 % in Fig. 7b. Good results indicated an efficient and reproducible immobilization process for AO on the surface of the biocompatible-conducting PEDOT composite matrix. The excellent repeatability and reproducibility of the fabricated AO composite modified electrode demonstrated the high stability of the fabricated AO composite modified electrode and the controllable process for the amounts of enzyme. EMIES, SLS, MWCNTs, and Nafion provided the biocompatible environment for maintaining the bioactivity of biologically active AO molecules on the conducting PEDOT composite matrix. MWCNT–Nafion composite film improved the stability of biosensing devices.

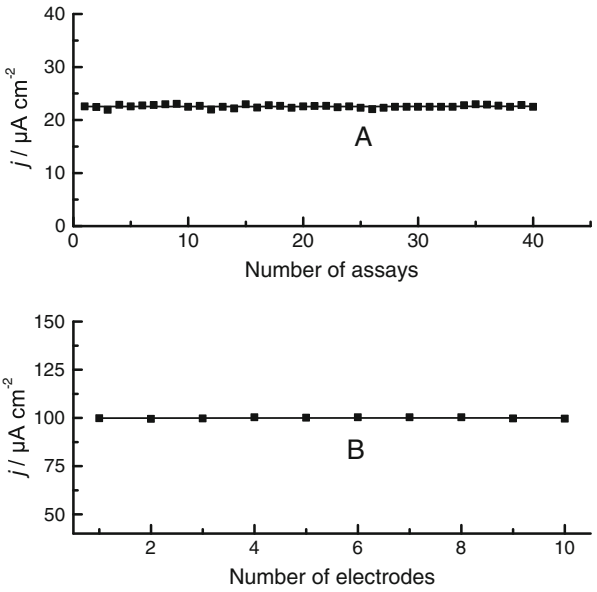

Fig. 7 The operational stability of the fabricated sandwich-type AO composite modified electrode

Specificity of AO Composite Modified Electrode

Different substances were used for studying the specificity of the fabricated sandwich-type AO composite modified electrode. The solution was allowed to stir at a constant speed of 300 rpm. The *I–t* curve in Fig. 8 demonstrated that the addition of 0.1 mM VC caused a noticeable change in current response, while the successive addition of 1 mM different

Interferents	Relative activity (%) chronoamperometric method 0.1 mM Interferents	1 mM Interferents	Interferents	Relative activity (%) chronoamperometric method 0.1 mM Interferents	1 mM Interferents
Glucose (a)	0.00	0.00	Urea (h)	0.00	0.00
Fructose (b)	0.00	0.00	Mannite(i)	0.00	0.00
Sucrose (c)	0.00	0.00	Oxalic acid (j)	0.00	0.00
L-Aspartic acid (d)	0.00	0.00	Citric acid (k)	0.00	0.00
DL-Alanine (e)	0.00	0.00	Sorbierite (l)	0.00	0.00
DL-Malic acid (f)	0.00	0.00	L-Glycine (m)	0.00	0.00
Nicotinic acid (g)	0.00	0.00	Inositol (n)	0.00	0.00

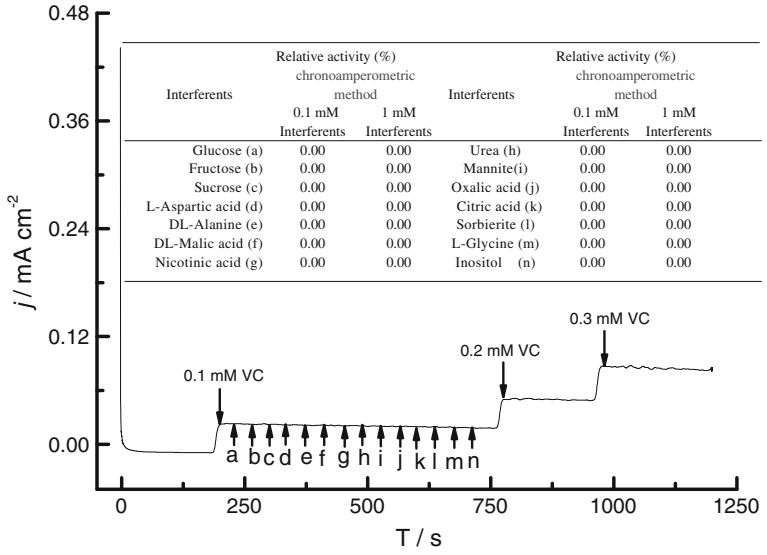

Fig. 8 The *I–t* curve of the fabricated sandwich-type AO composite modified electrode in constant VC solutions containing 1 mM different substances. Inset: the specificity of AO composite modified electrode in different interferents

compounds did not cause an obvious change in current response, indicating that the fabricated AO composite modified electrode had a good anti-interference ability, and AO molecules and Nafion film provided a good selectivity for the determination of VC. In addition, the current response of the fabricated AO composite modified electrode was determined in PBS containing the constant VC and 1 mM different interferents. The degree of interference was calculated according to the equation as follows:

$$D_{\text{inter}} = \frac{I_{\text{total}} - I_{\text{VC}}}{I_{\text{total}}} \tag{2}$$

where I_{total} is the total current response of the fabricated AO composite modified electrode for bioelectrocatalytic oxidation of VC in the constant VC solutions containing different interferents with the concentration of 1 mM, and I_{vc} is the current response of the fabricated AO composite modified electrode for bioelectrocatalytic oxidation of VC in the constant VC solution without interferents. Results were presented in Fig. 8 inset, indicating that these interferents did not cause significant interference in current response of the fabricated AO composite modified electrode. Hence, the fabricated sandwich-type composite AO composite modified electrode had good specificity.

Application in Real Samples Analysis

Table 1 gives analytical results for the determination of VC in commercial juices. Values determined by the fabricated biosensor were in good agreement with that given by manufacturers, which demonstrated the feasibility and reliability of the present method. Therefore, good results also indicated that the fabricated biosensor could be employed for the determination and analysis of VC in agricultural crops in the near future.

Conclusion

The sandwich-type AO composite modified electrode was successfully prepared for determining the content of VC in commercial juices. EMIES, SLS, MWCNTs, and Nafion could

Table 1 The determination of VC in commercial juices using the fabricated sandwich-type AO composite modified electrode

Commercial drinks	[VC] (mg/100 mL)	[VC] by amperometric method (mg/100 mL)[a]	
		Mean±SD	RSD (%)
Fruit blend	10	9.3±0.5	5.4
Orange juice	13	12.51±0.3	2.7
Grape juice	10	9.5±0.2	2.5
Vitamin water	20	19.4±0.6	2.8
Minute maid	7.5	7.4±0.3	3.9
Lemon juice	22.5	21.7±0.5	2.3
Mizone	20	19.5±1.0	5.0
Orangeate	5.6	5.5±0.2	3.5

SD standard deviation, *RSD* relative standard deviation

[a] Average values of five replications

improve the biocompatibility of film and provide the biocompatible environment for maintaining the bioactivity of biologically active AO molecules. EMIES and MWCNTs could effectively promote the direct electron transfer between AO molecules and PEDOT-modified electrode interface and improve the sensitivity and stability of AO-based biosensor. The synergistic electrocatalytic effect of MWCNTs also could enhance the bioelectrocatalytic performance of the AO-based biosensor. Nafion and MWCNTs with network structures are very beneficial for facilitating the immobilization of biologically active AO molecules and preventing its possible leakage from the electrode surface. The fabricated AO composite modified electrode demonstrated very low working potential, wide linear range, fast current response, low detection limit, high sensitivity, high bioaffinity, and bioactivity. Good results of VC determination in commercial juices indicated that the fabricated sandwich-type AO composite modified electrode will benefit subsequent determination of VC in agricultural crops. Meanwhile, the biocompatible inner film and the high stable and selective outer film will be a good candidate for the design of sensing and biosensing devices.

Acknowledgments NSFC (50963002 and 51073074), Key Projects in the National Science & Technology Pillar Program in the Eleventh Five-Year Plan Period (2006BAD02A04, 2006BAD01A01), Jiangxi Provincial Department of Science and Technology (2006BAD01A01-2-5), Jiangxi Provincial Department of Education (GJJ11590 and GJJ10678), Natural Science Foundation of Jiangxi Province (2010GZH0041), and Key Laboratory of Photochemical Conversion and Optoelectronic Materials, TIPC, are acknowledged for their financial support.

References

1. Yang, W., Ratinac, K. R., Ringer, S. P., Thordarson, P., Gooding, J. J., & Braet, F. (2010). *Angewandte Chemie International Edition, 49*, 2114–2138.
2. Malhotra, B. D., Singhal, R., Chaubey, A., Sharma, S. K., & Kumar, A. (2005). *Current Applied Physics, 5*, 92–97.
3. Malhotra, B. D., Chaubey, A., & Singh, S. P. (2006). *Analytica Chimica Acta, 578*, 59–74.
4. Gerard, M., Chaubey, A., & Malhotra, B. D. (2002). *Biosensors and Bioelectronics, 17*, 345–359.
5. Groenendaal, B. L., Jonas, F., Freitag, D., Pielartzik, H., & Reynolds, J. R. (2000). *Advanced Materials, 12*, 481–494.
6. Groenendaal, L. B., Zotti, G., Aubert, P. H., Waybright, S. M., & Reynolds, J. R. (2003). *Advanced Materials, 15*, 855–879.
7. Kirchmeyer, S., & Reuter, K. (2005). *Journal of Materials Chemistry, 15*, 2077–2088.
8. Elschner, A., Kirchmeyer, S., Lövenich, W., Merker, U., & Reuter, K. (2010). *PEDOT: Principles and applications of an intrinsically conductive polymer*. Boca Raton: CRC.
9. Sakmeche, N., Aeiyach, S., Aaron, J. J., Jouini, M., Lacroix, J. C., & Lacaze, P. C. (1999). *Langmuir, 15*, 2566–2574.
10. Tsakova, V., Winkels, S., & Schultze, J. W. (2000). *Electrochimica Acta, 46*, 759–768.
11. Zhang, S. S., Hou, J., Zhang, R., Xu, J. K., Nie, G. M., & Pu, S. Z. (2006). *European Polymer Journal, 42*, 149–160.
12. Morán, M. C., Pinazo, A., Pérez, L., Clapés, P., Angelet, M., Garcia, M. T., et al. (2004). *Green Chemistry, 6*, 233–240.
13. Nnanna, I. A., & Xia, J. (2001). *Protein-based surfctants: synthesis, physicchemical properties and applications*. NewYork: Marcel Dekker.
14. Clapes, P., & Infante, M. R. (2002). *Biocatalysis and Biotransformation, 20*, 215–233.
15. Wen, Y. P., Xu, J. K., He, H. H., Lu, B. Y., Li, Y. Z., & Dong, B. (2009). *Journal of Electroanalytical Chemistry, 63*, 449–458.
16. Dobbelin, M., Marcilla, R., Pozo-Gonzalo, C., & Mecerreyes, D. (2010). *Journal of Materials Chemistry, 20*, 7613–7622.
17. Randriamahazaka, H., Plesse, C., Teyssié, D., & Chevrot, C. (2005). *Electrochimica Acta, 504*, 222–4229.

18. Randriamahazaka, H., Plesse, C., Teyssié, D., & Chevrot, C. (2003). *Electrochemistry Communications, 5*, 613–617.
19. Ahmad, S., Deepa, M., & Singh, S. (2007). *Langmuir, 23*, 11430–11433.
20. Santhosh, P., Manesh, K. M., Uthayakumar, S., Komathi, S., Gopalan, A. I., & Lee, K. P. (2009). *Bioelectrochemistry, 75*, 61–66.
21. Serafín, V., Agüí, L., Yáñez-Sedeño, P., & Pingarrón, J. M. (2010). *Journal of Electroanalytical Chemistry, 656*, 152–158.
22. Dong, B., Zhang, S. S., Zheng, L. Q., & Xu, J. K. (2008). *Journal of Electroanalytical Chemistry, 619–620*, 193–196.
23. Holbrey, J. D., Reichert, W. M., Swatloski, R. P., Broker, G. A., Pitner, W. R., Seddon, K. R., et al. (2002). *Green Chemistry, 4*, 407–413.
24. Tan, Y. Y., Guo, X. X., Zhang, J. H., & Kan, J. Q. (2010). *Biosensors and Bioelectronics, 25*, 1681–1687.
25. Ndiaye, C., Xu, S. Y., & Wang, Z. (2009). *Food Chemistry, 113*, 92–95.
26. Li, S., Tan, Y., Wang, P., & Kan, J. Q. (2010). *Sensors and Actuators B: Chemical, 144*, 18–22.
27. Jiang, Y., Wang, A., & Kan, J. Q. (2007). *Sensors and Actuators B: Chemical, 124*, 529–534.
28. Wen, Y. P., Duan, X. M., Xu, J. K., Yue R. R., Li, D., Liu M., Lu, L. M., & He, H. H. (2012). *Journal of Solid State Electrochemistry* (accepted).
29. Wang, J. (2005). *Electroanalysis, 17*, 7–14.
30. Ahammad, A. J., Lee, J. J., & Rahman, M. (2009). *Sensors-basel, 9*, 2289–2319.
31. Zengin, H., Zhou, W., Jin, J., Czerw, R., Smith, D. W., Jr., Echegoyen, L., et al. (2002). *Advanced Materials, 14*, 1480–1483. 464.
32. Wei, Z., Wan, M., Lin, T., & Dai, L. (2003). *Advanced Materials, 15*, 136–139.
33. Santhosh, P., Gopalan, A., & Lee, K. P. (2006). *Journal of Catalysis, 238*, 178–185.
34. Yang, M. H., Jiang, J. H., Yang, Y. H., Chen, X. H., Shen, G. L., & Yu, R. Q. (2006). *Biosensors and Bioelectronics, 21*, 1791–1797. 468.
35. Liu, M., Wen, Y. P., Li, D., He, H. H., Xu, J. K., Liu, C. C., et al. (2011). *Journal of Applied Polymer Science, 122*, 1142–1142. 470.
36. Liu, M., Wen, Y. P., Xu, J. K., He, H. H., Li, D., Yue, R. R., et al. (2011). *Analytical Sciences, 27*, 477–482.
37. Wang, J., Musameh, M., & Lin, Y. (2003). *Journal of the American Chemical Society, 125*, 2408–2409.
38. Tsai, Y. C., & Shiu, C. C. (2007). *Sensors and Actuators B: Chemical, 125*, 10–16.
39. Tsai, Y. C., Chen, J. M., Li, S. C., & Frank, M. (2004). *Electrochemistry Communications, 6*, 917–922.
40. Xu, J. J., Yu, Z. H., & Chen, H. Y. (2002). *Analytica Chimica Acta, 463*, 239–247.
41. Moore, C. M., Akers, N. L., Hill, A. D., Johnson, Z. C., & Minteer, S. D. (2004). *Biomacromolecules, 5*, 1241–1247.
42. Liang, Z. X., Zhao, T. S., & Prabhuram, J. (2006). *Journal of Electrochimica Acta, 51*, 6412–6418.
43. Karyakin, A. A., Kotelnikova, E. A., Lukachova, L. V., Karyakina, E. E., & Wang, J. (2002). *Analytical Chemistry, 74*, 1597–1603.
44. Messerschmidt, A., & Huber, R. (1990). *European Journal of Biochemistry, 187*, 341–352. 481.
45. Messerschmidt, A., Ladenstein, R., Huber, R., Bolognesi, M., Avigliano, L., Petruzzelli, R., et al. (1992). *Journal of Molecular Biology, 224*, 179–205.
46. Carvalho, L. B., Lima, C. J., & Medeiros, P. H. (1981). *Phytochemistry, 20*, 2423–2424.
47. Farver, O., Wherland, S., & Pecht, I. (1994). *Journal of Biological Chemistry, 269*, 22933–22936.
48. Wen, Y. P., Lu, L. M., Li, D., Liu, M., He, H. H., & Xu, J. K. (2012). *Chinese Chemical Letters, 23*, 221–224.
49. Liu, M., Wen, Y., Li, D., Yue, R., Xu, J., & He, H. (2011). *Sensors and Actuators B: Chemical, 159*, 277–285.
50. Chauhan, N., Priyanka, T. D., & Pundir, C. S. (2010). *Journal of Molecular Catalysis B: Enzymatic, 67*, 66–71.
51. Sezgintürk, M. K., Koca, H. B., Özben, Y. S., & Dinkaya, E. (2010). *Artificial Cells, Blood Substitutes, 38*, 215–221.
52. Chauhan, N., Narang, J., & Pundir, C. S. (2011). *Analyst, 136*, 1938–1945.
53. Marangoni, A. (2003). *Enzyme kinetics: A modern approach*. Chichester: Wiley.
54. Limoges, B., Marchal, D., Mavré, F., & Savéant, J. M. (2006). *Journal of the American Chemical Society, 128*, 2084–2092.
55. Limoges, B., Marchal, D., Mavré, F., & Savéant, J. M. (2008). *Journal of the American Chemical Society, 130*, 7276–7285.
56. Shu, F., & Wilson, G. (1976). *Analytical Chemistry, 48*, 1679–1686.
57. Kamin, R., & Wilson, G. (1980). *Analytical Chemistry, 52*, 1198–11205.